

# Mathematical Modeling and Optimization of Tribological Properties of AA7075-T6 Using Taguchi and Multi Response Performance Index Approaches

Srinivasulu Reddy Kunduru<sup>1\*</sup>, Krishna Mohan Reddy Kunduru<sup>2</sup>, Jayakiran Reddy Esanakula<sup>1</sup> and Nitish Reddy Pasham<sup>1</sup>

<sup>1</sup>Department of Mechanical Engineering, Sreenidhi Institute of Science and Technology, Hyderabad, Telangana, India

<sup>2</sup>Engineering Design Department, Overhead Door Corporation, Texas, USA

## \*Correspondence to:

Srinivasulu Reddy Kunduru  
Department of Mechanical Engineering,  
Sreenidhi Institute of Science and Technology,  
Hyderabad, Telangana, India.  
E-mail: [k.srinivasulureddy@gmail.com](mailto:k.srinivasulureddy@gmail.com)

Received: September 15, 2023

Accepted: November 24, 2023

Published: November 29, 2023

**Citation:** Kunduru SR, Kunduru KMR, Esanakula JR, Pasham NR. 2023. Mathematical Modeling and Optimization of Tribological Properties of AA7075-T6 Using Taguchi and Multi Response Performance Index Approaches. *NanoWorld J* 9(S4): S300-S304.

**Copyright:** © 2023 Kunduru et al. This is an Open Access article distributed under the terms of the Creative Commons Attribution 4.0 International License (CCBY) (<http://creativecommons.org/licenses/by/4.0/>) which permits commercial use, including reproduction, adaptation, and distribution of the article provided the original author and source are credited.

Published by United Scientific Group

## Abstract

Usage of lightweight materials with better tribological characteristics is significantly increasing in industrial applications. Current research work is focusing on optimizing the tribological properties of AA7075-T6 alloy. Tribological properties wear rate (WR) and coefficient of friction (COF) of AA7075-T6 are found using pin-on-disk apparatus. Initially, an L9 orthogonal array as per Taguchi method is used to design the number of experiments. To optimize both wear rate and COF properties, in the present research work multi response performance index (MRPI) method is used.

## Keywords

Tribological properties, AA7075-T6, Taguchi, Multi response performance index

## Introduction

Aluminum alloys like 7000 and 6000 grades are widely used in several applications because of strength to weight ratio is high and very good corrosion resistance property. The density of aluminum is 2.7 g/cm<sup>3</sup> which is very low compared to the density of steel which is 7.87 g/cm<sup>3</sup>. Aluminum alloys of these series are lighter, almost one third of steel. Aluminum 7075-T6 alloy in terms of toughness and specific strength are more or less equal to certain steels. Apart from this, aluminum alloys have good economic value and are relatively cost-effective when compared to steels [1].

The current study is aimed to find the optimal settings during the tribological performance of AA7075-T6 alloy which is acting as pin and sliding against a pin-on-disk testing machine and the disk is made up of stainless steel. The wear behaviour of the specimen is studied by measuring the wear of the worn surface specimens and coefficient of friction values are recorded by the tester during the experiment. Low contact loads and small sliding velocities are selected intentionally to eliminate the thermal influence during experimentation. Various research has conducted experiments on AA7075 alloy reinforced with silicon carbide, boron carbide, carbon nanotubes, graphene and titanium carbide and reported improvement in wear properties of AA7075 alloy with these reinforcements [2-4]. Much work is not reported on the wear behavior of AA7075-T6 alloy (Tempered 7075 aluminum alloy with major alloying element zinc). Hence this investigation is carried out to find the optimum conditions for better WR and COF of this alloy using Taguchi method and multi response performance index method coupled with Taguchi method is methods [5-7].

The majority of research in this area have used aluminum metal or 7000 and 6000 series of aluminum alloys as the primary material in the military and

aviation industries, ushering in a new era of creating composite materials to get around the biggest obstacle, namely, weak tribological qualities. This study examined the effects of incorporating nanofillers into hybrid composite laminates comprised of epoxy, basalt fabric, fiber made by woven Kevlar, and aluminum plates of AA7075-T6 using STF because of the significant role that aluminum plays in the defense industry. The final hybrid laminate's capacity to absorb energy and respond to ballistics has been researched. A laminate without any nanofillers and a hybrid composite laminate infused with different nanofillers, such as, magnesium hydroxide, aluminum oxide, silicon dioxide, and flour of tapioca, were studied and compared for their impact resistance under a ballistic load.

A pressure tank, compressor with high horsepower and a stiff conical shaped bullet (15 g in mass and diameter of 8.5 mm) will be used in an air cannon to investigate the effects of direction of fiber, densities, and the limit of ballistic on the hybrid composites' ability to dissipate energy. Atrian et al. [8] tested aramid, basalt, and epoxy resin in various ways. Six different specimens, each 10 cm, 10 cm, and 3.5 mm thick, were made by alternately stacking the non-hybrid and hybrid orientations of the Kevlar fibers and basalt. It was discovered that the average ballistic resistance rate of sandwich hybrids and interpenetrating hybrids was higher than that of pure basalt. In comparison to pure Kevlar, energy absorption was increased by around 11.3% for sandwich hybrids and around 21.7% for interpenetrating hybrids. Basalt and Kevlar work together to provide a resistance to high-velocity impacts that surpasses that of any single material. Anderson and Dannemann [9] looked into how the 6061-T6 and aluminum alloys 7075-T6 behaved in terms of energy absorption. Each of the 10 targets was constructed from around 10 7075-T6 and 6061-T6 aluminum plates. Al-6061-T6 and Al-7075-T6 were subjected to a ballistic impact test, with the hitting velocity varied between 370 and 270 m/s. The findings show that Al-7075-T6 is more impact-resistant than Al-6061-T6. The usage of calcium carbonate, nano-silica, silicon carbide, graphene oxide, and carbon nanotubes, according to Demircioglu et al. [10], enhances friction force much more than thickening of shear. Vacuum-assisted resin transfer molding, without or with nanoparticles, was used to create the sample panels. The addition of aluminum, alumina, graphene oxide, colloidal silica, silicon carbide, nano-clay and potato flour increased the ballistic performance of a composite material formed of fibers of Kevlar and polymer.

Haro et al. [11] used colloidal silica, gamma alumina, silicon carbide, potato flour, aluminum, and as nano-fillers. The final product of size 150 mm x 150 mm samples was compressed after the Kevlar fibers with 20 layers were manually placed down. Due to the nanofillers' effective coverage of the fiber surfaces and sealing of the gaps between the bundles of fiber, the resistive capacity of the laminates was higher than that of the hybrid targets created with potato vegetable flour, according to an analysis of their microstructure. Naveen et al. [12] tested the incorporation of graphene nanoplatelets (GnPs) into epoxy utilizing *Cocos nucifera* sheath, Kevlar 29, ultra-sonification and epoxy resin. The structures of the specimens were made with laminates of 12 layers of sheath sheets of *C. nucifera* and 9 layers of Kevlar, respectively. These lam-

inates were then manually laid up and compacted using the technique of compression molding. Limit velocity can be reduced by GnPs of epoxy laminates reinforced with *C. nucifera* sheath while increasing the limit velocity of epoxy laminates reinforced with Kevlar. Though surface connections between the GnP-modified epoxy matrix and fiber were strengthened by adding GnPs, this substance is still not suitable for capturing and kinetic energy dispersion of the projectile. Using epoxy resin of the DGEBA type, de Mendonça Neuba et al. [13] studied the *Cyperus malaccensis* sedge. Ballistic impact remained unchanged, tensile strength declined, Young's modulus rose, and impact energy (Izod) rose. This showed that the fibers mostly served as poor interface defects of fiber-matrix. The studies were conducted by Filho et al. [14] using epoxy resin and piassava fiber. This structure was made up of specimens that ranged in size from 60 mm to 75 mm and included 10 to 30 percent piassava fiber by volume. The ballistic impact maintains a velocity of 200 - 240 m/s, and the piassava fiber composite of 10 vol.% exhibits the maximum level of energy absorption among all situations tested. As a result, it is ideal for usage as one of several components rather than the only one in an armor system.

## Materials and Method

### Materials

AA7075-T6 (heat-treated) alloy in the form of rods are taken to find the properties like WR and COF in this research work. Various elements present in this AA7075-T6 alloy are presented in table 1.

### Wear test

An instrument which will monitor and measure the friction and wear is used to find the wear behavior in dry. 30 mm height with 8 mm diameter standard wear pin specimens are prepared from AA7075(T6) alloy and polished metallographically for wear test. Experiments are conducted by changing the parameters applied load, sliding distance travelled and velocity at which sliding takes place. These three factors are tested at three levels. Design of experiment by Taguchi approach is used to perform the experiments. As per Taguchi method, L9 orthogonal array is used and nine experiments are conducted by varying load applied at 30, 20, and 10 N and velocity of sliding at 2.61, 2.09, and 1.57 m/s and distance of sliding at 3000, 2000, and 1000 meters. At all these nine levels, COF values are directly taken from the system data and wear rates are found by measuring the difference in weights of the

Table 1: Weight % of AA7075 alloy composition.

S. No.	Element	Composition % in AA7075
1	Magnesium	2.4
2	Manganese	0.06
3	Titanium	0.07
4	Copper	1.5
5	Silicon	0.08
6	Ferrite	0.24
7	Chromium	0.20
8	Zinc	5.8
9	Aluminum	Remaining

specimen before and after the test. In table 2, experimental results are presented.

## Results and Discussion

As per Taguchi design, the two responses COF and WR are to be as small as possible for optimization of static problems. The signal to noise (S/N) ratio for smaller the better characteristic is calculated using equation 1.

$$\frac{S}{N} \text{ ratio} = -10 * \log \left( \sum \frac{Y^2}{n} \right) \quad (1)$$

Where, number of repetitions is n and response value is y.

### Optimization of WR

L9 array design is given in table 3. Main effects plot of S/N ratios of WR is shown in figure 1. From figure 1, it is observed that load at level 1, velocity of sliding at level 3 and distance of sliding at level 1 are optimum for low WR. The ranking of the three factors on WR is shown in table 4. Predicted mean WR at the optimum levels is calculated as per Taguchi methodology and found to be 0.4146. Prediction of mean values of wear and S/N ratio are given in table 5.

### Optimization of COF

L9 array design is given in table 6 and ranking of factors are presented in table 7. As per the ranking table, load applied is the first factor which will have impact on COF. The other two in the order of priority are sliding velocity and distance of sliding, respectively. Main effects graph is shown in figure 2 and predicted COF is 1.05275 and shown in table 8. Prediction of mean and ratio of S/N mentioned above are presented in table 8.

### Multi response optimization using MRPI method

To optimize one response each time, Taguchi Method is best suited in many cases. Here the current more than one

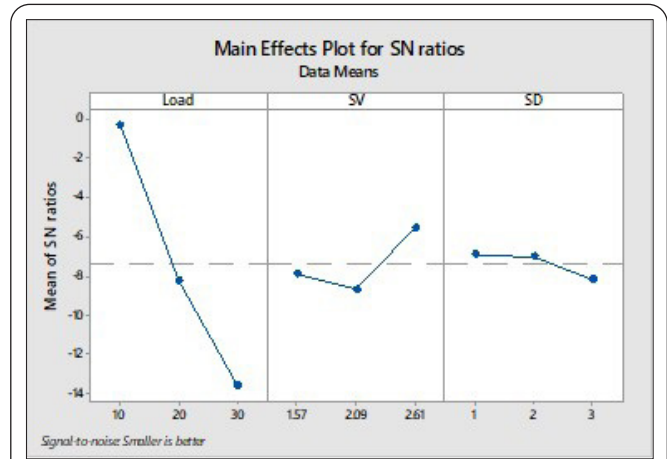


Figure 1: Main effects plot for WR.

Table 4: Ranking of factors on WR.

Level	Load	SV	SD
1	-0.2900	-7.9120	-6.9035
2	-8.2338	-8.6801	-7.0232
3	-13.6059	-5.5376	-8.2030
Delta	13.3160	3.1425	1.2995
Rank	1	2	3

Table 5: Prediction of wear.

S/N ratio	Mean
2.02203	0.414673

Table 6: Taguchi orthogonal array for COF.

Taguchi array	L9 (3 <sup>3</sup> )
Factors	3
Runs	9

Table 7: Ranking of factors on COF.

Level	Load	SV	SD
1	-4.735	-13.355	-13.115
2	-14.803	-13.582	-13.456
3	-18.684	-11.285	-11.651
Delta	13.950	2.296	1.806
Rank	1	2	3

response problem is converted as one response problem which is called MRPI and this MRPI response is optimized using larger the better-quality characteristic as per Taguchi method.

$$\text{MRPI} = W1 \times (\text{WR}) + W2 \times (\text{COF}) \quad (2)$$

Where, W1 is the weightage of first response (WR) and W2 is weightage of second response (COF), which are calculated using the equation 3 and 4, respectively.

$$W1 = (1/\text{WR}) / (\sum(1/\text{WR})) \times \text{WR} \quad (3)$$

$$W2 = (1/\text{COF}) / (\sum(1/\text{COF})) \times \text{COF} \quad (4)$$

Table 2: WR and COF values.

S. No.	Applied Load (N)	Sliding velocity (m/s)	Sliding distance (km)	WR (mm <sup>3</sup> /m)	COF
1	10	1.57	1	0.70106474	1.883
2	10	2.09	2	1.2267788	2.277754
3	10	2.61	3	1.28519687	1.196419
4	20	1.57	2	3.68033649	5.956882
5	20	2.09	3	2.2198855	5.204497
6	20	2.61	1	2.10304942	5.357789
7	30	1.57	3	5.95864003	8.981911
8	30	2.09	1	7.36067298	9.190862
9	30	2.61	2	2.50508237	7.690329

Table 3: Taguchi orthogonal array for wear test.

Taguchi orthogonal array	L9 (3 <sup>3</sup> )
Factors	3
Runs	9

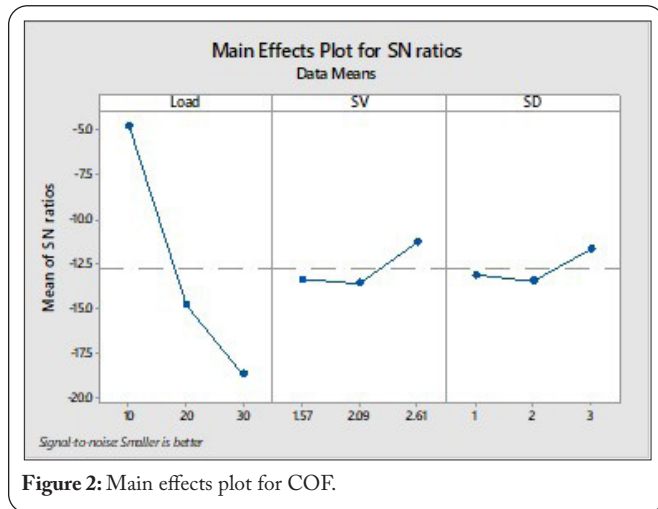


Figure 2: Main effects plot for COF.

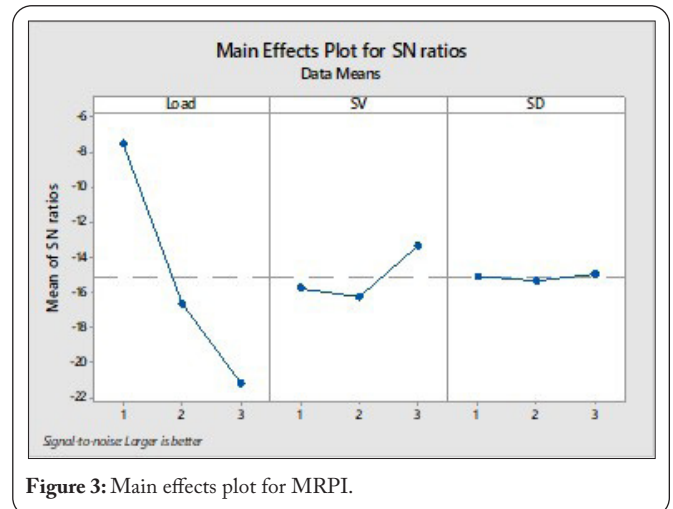


Figure 3: Main effects plot for MRPI.

Table 8: Predicted mean and S/N of COF.

S/N ratio	Mean
-2.18993	1.05275

Table 5 shows the calculation of MRPI. Among the MRPI values shown in table 9, experiment number 1 has highest rank and Taguchi method is to optimize the larger-the-better MRPI value. S/N ratios for larger-the-better criteria are calculated using equation 5.

$$\frac{S}{N} \text{ ratio} = -10 \log_{10} \left( \frac{1}{n} \right) \sum_{i=1}^n \frac{1}{y_i^2} \quad (5)$$

From the main effects graph for S/N ratios of MRPI shown in figure 3, it is clear that level 1 of load, level 3 of sliding velocity and level 3 of sliding distance are optimum conditions which will satisfy both WR and COF, using MRPI method. Results of single response optimization problem using Taguchi methodology and optimization of multi responses using MRPI coupled with Taguchi methodology are compared in table 10.

Among the three different settings of load, sliding velocity and sliding distance (10,2.61,1; 10,2.61,2 and 10,2.61,3)

experiment with (10,2.61,3) is suggested by MRPI coupled with Taguchi method for the multi response optimization, which is already conducted as part of Taguchi L9 orthogonal array which is experiment number 3.

## Conclusion

From the results comparison table 6, it can be concluded that MRPI method can be used to optimize the multi response optimization problems and Taguchi methodology can be applied to optimize the MRPI values. Levels suggested by single response and multi response optimization methods are experimentally validated and presented in table 10. From the results it can be stated that multi response optimization is achieved with the compromise in one of the two responses. In this case, WR is compromised.

## Acknowledgements

None.

## Conflict of Interest

None.

Table 9: Calculation of multi response performance index.

Trail No.	WR	COF	1/WR	W1	1/COF	W2	MRPI
1	0.70106	1.883	1.426402	0.289908	0.531067	0.196491	0.486399
2	1.22678	2.27775	0.815143	0.165673	0.439029	0.162438	0.328111
3	1.2852	1.19642	0.778091	0.158142	0.835828	0.30925	0.467393
4	3.68034	5.95688	0.271714	0.055224	0.167873	0.062112	0.117336
5	2.21989	5.2045	0.450474	0.091556	0.192142	0.071091	0.162647
6	2.10305	5.35779	0.4755	0.096643	0.186644	0.069057	0.1657
7	5.95864	8.98191	0.167824	0.034109	0.111335	0.041193	0.075302
8	7.36067	9.19086	0.135857	0.027612	0.108804	0.040257	0.067869
9	2.50508	7.69033	0.399188	0.081133	0.130033	0.048111	0.129244
Sum	27.04071	47.73944	4.920193		2.702755		



**Table 10:** Results comparison of various MCDM methods.

	Taguchi (WR)	Taguchi (COF)	MRPI coupled with Taguchi
Criteria	Smaller the better	Smaller the better	Larger the better
Levels suggested for (Load, sliding velocity, and sliding distance)	10, 2.61, 1 (Not part of L9 array)	10, 2.61, 3 (Exp. No. 3)	10, 2.61, 3 (Exp. No. 3)
Predicted value	0.414673	1.05275	NA
Experimental values	0.435865	1.196419	WR: 1.285196; COF: 1.196419

## References

- Lal S, Sehrawat R, Sharma N. 2023. A short review on the developments of aluminium matrix composites. *Mater Today Proc* 1-8. <https://doi.org/10.1016/j.matpr.2023.02.012>
- Rafi SM, Kumar TS, Thankachan T, Selvan CP. 2023. Synergistic effect of FSP and TiB<sub>2</sub> on mechanical and tribological behavior of AA2024 surface composites. *J Tribol* 145(11): 114501. <https://doi.org/10.1115/1.4062517>
- Kumar P, Kumar B. 2023. Effect of T6 heat treatment on mechanical and tribological properties of fabricated AA7075/ZrB<sub>2</sub>/fly ash hybrid aluminum metal matrix composite by ultrasonic-assisted stir casting enroute. *Int J Metalcast* 1-19. <https://doi.org/10.1007/s40962-023-01177-5>
- Bharathi P, Kumar TS. 2023. Effect of silicon carbide and boron carbide on mechanical and tribological properties of aluminium 7075 composites for automobile applications. *Silicon* 15: 6147-6171. <https://doi.org/10.1007/s12633-023-02498-0>
- Adib MH, Abedinzadeh R. 2023. Study of mechanical properties and wear behavior of hybrid Al/(Al<sub>2</sub>O<sub>3</sub> + SiC) nanocomposites fabricated by powder technology. *Mater Chem Phys* 305: 127922. <https://doi.org/10.1016/j.matchemphys.2023.127922>
- Aghajani S, Pouyafar V, Meshkabadi R, Volinsky AA, Bolouri A. 2023. Mechanical characterization of high volume fraction Al7075-Al<sub>2</sub>O<sub>3</sub> composite fabricated by semisolid powder processing. *Int J Adv Manuf Technol* 125(5-6): 2569-2580. <https://doi.org/10.1007/s00170-023-10881-9>
- Khalid MY, Umer R, Khan KA. 2023. Review of recent trends and developments in aluminium 7075 alloys and metal matrix composites (MMCs) for aircraft applications. *Results Eng* 20: 101372. <https://doi.org/10.1016/j.rineng.2023.101372>
- Atrian A, Majzoobi GH, Enayati MH, Bakhtiari H. 2014. Mechanical and microstructural characterization of Al7075/SiC nanocomposites fabricated by dynamic compaction. *Int J Miner Metall Mater* 21: 295-303. <https://doi.org/10.1007/s12613-014-0908-7>
- Anderson CE, Dannemann KA. 2002. Deformation and damage of two aluminum alloys from ballistic impact. *AIP Conf Proc* 620: 1298-1301. <https://doi.org/10.1063/1.1483777>
- Demircioglu TK, Balikoglu F, Beyaz S, Bülbül B. 2021. Effect of lead metaborate as novel nanofiller on the ballistic impact behavior of Twaron (R)/epoxy composites. *Compos Commun* 27: 100832. <https://doi.org/10.1016/j.coco.2021.100832>
- Haro EE, Odeshi AG, Szpunar JA. 2016. The energy absorption behavior of hybrid composite laminates containing nano-fillers under ballistic impact. *Int J Impact Eng* 96: 11-12. <https://doi.org/10.1016/j.ijimpeng.2016.05.012>
- Naveen J, Jawaid M, Zainudin ES, Sultan MTH, Yahaya R. 2019. Effect of graphene nanoplatelets on the ballistic performance of hybrid Kevlar/Cocos nucifera sheath-reinforced epoxy composites. *Text Res J* 89(21-22): 4349-4362. <https://doi.org/10.1177/0040517519833970>
- de Mendonça Neuba L, Junio RFP, Souza AT, Carvalho MT, Ribeiro MEA, et al. 2023. Dynamic mechanical and thermal mechanical analysis of *Cyperus malaccensis* sedge fiber reinforced GO-incorporated epoxy nanocomposites: a short communication. *J Mater Res Technol* 24: 1653-1662. <https://doi.org/10.1016/j.jmrt.2023.03.075>
- Filho FCG, Oliveira MS, Pereira AC, Nascimento LFC, Matheus JRG, et al. 2020. Ballistic behavior of epoxy matrix composites reinforced with piassava fiber against high energy ammunition. *J Mater Res Technol* 9(2): 1734-1741. <https://doi.org/10.1016/j.jmrt.2019.12.004>